Balkan Med J 2024;41:213-21

Radiological Features for Predicting the Status of CD8-Positive Lymphocytes in HER2 Positive Breast Cancer

Yuhong Fan[1]*, Xiaoguang Li[2]*, Peng Zhong[3], Hong Guo[2], Dong Han[1], Wuguo Tian[4], Jingqin Fang[1]

[1]Department of Ultrasound Diagnosis, Daping Hospital, Army Medical University, Chongqing, China
[2]Department of Radiology, Daping Hospital, Army Medical University, Chongqing, China
[3]Department of Pathology, Daping Hospital, Army Medical University, Chongqing, China
[4]Department of Breast and Thyroid Surgery, Daping Hospital, Army Medical University, Chongqing, China
Contributed equally

Background: The level of tumor-infiltrating lymphocytes (TILs) in human epidermal growth factor receptor type 2 (HER2)-positive breast cancer (BC) is positively correlated with pathological complete response.

Aims: To investigate the relationship between ultrasound (US) and magnetic resonance imaging (MRI) features and the level of CD8-positive TILs ($CD8^+$-TILs) in patients with HER2-positive BC.

Study Design: Retrospective cohort study.

Methods: This retrospective study included 155 consecutive women with HER2-positive BC. Patients were divided into two groups: $CD8^+$-TIL_{low} (< 35%) and $CD8^+$-TIL_{high} (≥ 35%) groups. US and MRI features were evaluated using the BI-RADS lexicon, and the apparent diffusion coefficient (ADC) value was calculated using RadiAnt software. Univariate and multivariate analyses revealed the optimal US and MRI features for predicting $CD8^+$-TIL levels. Receiver operating characteristic analysis and the Delong test were used to compare the diagnostic performance of US and MRI features. Furthermore, implementing a nomogram will increase clinical utility.

Results: Univariate analysis of US features showed significant differences in shape, orientation, and posterior echo between the two groups; however, there were no significant differences in margins, internal echo, and microcalcification. Multifactorial analysis revealed that shape, orientation, and posterior echo were independent risk factors, with odds ratios of 11.62, 2.70, and 0.16, respectively. In terms of MRI features, ADC was an independent predictor of $CD8^+$-TIL levels. These three US features and the ADC performed well, with area under the curve (AUC) values of 0.802 and 0.705, respectively. The combination of US and ADC values had higher predictive efficacy (AUC = 0.888) than either US or ADC alone ($p = 0.009$, US_ADC vs. US; $p < 0.001$, US_ADC vs. ADC).

Conclusion: US features (shape, orientation, and posterior echo) and ADC value may be a valuable tool for estimating $CD8^+$-TIL levels in HER2-positive BC. The nomogram may help clinicians in making decisions.

INTRODUCTION

Human epidermal growth factor receptor 2 (HER2) is overexpressed in 20%-30% of invasive breast cancers (BCs), which is associated with aggressive tumor biology and a poor prognosis.[1,2] Tumor-infiltrating lymphocytes (TILs) are a biomarker of lymphocyte-mediated immunity, particularly in HER2-positive and triple-negative BC.[2-4] TIL levels are positively correlated with clinical benefit in HER2-positive BC.[5-10] According to the fifth edition of the World Health Organization's classification of tumors, TIL quantification in HER2-positive subtypes was supported. Recent research suggests investigating the role of TIL subpopulations in HER2-positive BC.[1] TILs' anti-tumor effect is primarily mediated by CD8-positive lymphocytes. Extensive infiltration of CD8-positive lymphocytes is strongly associated with patient survival and treatment response.[11,12] Therefore, non-invasive prediction of CD8-positive lymphocyte status in HER2-positive BC could be useful in clinical settings.

Ultrasound (US) and magnetic resonance imaging (MRI) are both widely available and standard imaging modalities for detecting BC

Corresponding author: Jingqin Fang, Department of Ultrasound Diagnosis, Daping Hospital, Army Medical University, Chongqing, China

e-mail: jingqin0405@163.com

Received: February 17, 2024 **Accepted:** April 04, 2024 **Available Online Date:** May 02, 2024 • **DOI:** 10.4274/balkanmedj.galenos.2024.2024-2-64

Available at www.balkanmedicaljournal.org

ORCID iDs of the authors: Y.F. 0000-0001-5232-4478; X.L. 0000-0001-7410-4134; P.Z. 0000-0002-6966-8549; H.G. 0000-0002-9565-890X; D.H. 0000-0002-9495-3835; W.T. 0000-0001-6414-6808; J.F. 0000-0001-5521-1778.

Cite this article as: Fan Y, Li X, Zhong P, Guo H, Han D, Tian W, Fang J. Radiological Features for Predicting the Status of CD8-Positive Lymphocytes in HER2 Positive Breast Cancer. Balkan Med J.; 2024; 41(3):213-21.

and accessing therapeutic efficacy. Previous studies evaluating the relationship between US features and TIL levels found some correlations, such as tumor shape and internal echo.[13-16] MRI characteristics, such as tumor size, margin, apparent diffusion coefficient (ADC), and enhancement pattern, have been associated with TIL levels of BC.[1-5,10,11,14,17-24] However, no conclusive results were obtained.

To the best of our knowledge, no research has been conducted to investigate the relationships between multimodality (including US and MRI features) and $CD8^+$-TIL levels in HER2-positive BC and the complementary efficacy of these two routine imaging modalities in accessing $CD8^+$-TILs. In this study, we aim to identify the optimal US and MRI features for predicting $CD8^+$-TIL levels in HER2-positive BC and compare the predictive power of single imaging features versus combined imaging features.

MATERIALS AND METHODS

Patients

This study was approved by the Ethics Committee of Army Medical Hospital [approval number: 2023 (202)], and informed consent was waived due to the retrospective nature of the study. This study included 155 patients with pathologically confirmed HER2-positive BC between January 2019 and July 2022. The inclusion criteria were as follows: (a) age ≥ 18 yr; (b) primary US and MR images were available; (c) the interval time between US and MRI was within 2 weeks; and (d) pathologically confirmed HER2-positive BC. Patients were excluded if they performed any treatment before primary US and MRI examinations or had poor quality of US and MRI images. A flowchart for participant selection is shown in Figure 1.

US procedure and analysis

The DC8 US diagnostic system (Mindray Medical International Co., Ltd., Shenzhen, China) with a 3-12-MHz linear-array transducer was used in transverse and longitudinal planes for US examinations. Representative images of the largest diameter lesions were saved. According to the BI-RADS US lexicon, US features, such as shape, margin, orientation, size, internal echo, posterior echo change, and microcalcification, were examined by two radiologists with 3-5 yr of experience in breast US. The pathological results, including the subtype of the breast lesion and the level of $CD8^+$-TILs level, were kept blinded from two radiologists. If there is an inconsistency, the two radiologists will first negotiate and resolve the issue, otherwise, another physician with 10 yr of experience in breast US screening will determine the result. When multiple BC masses were present, the largest BC mass was selected for analysis.

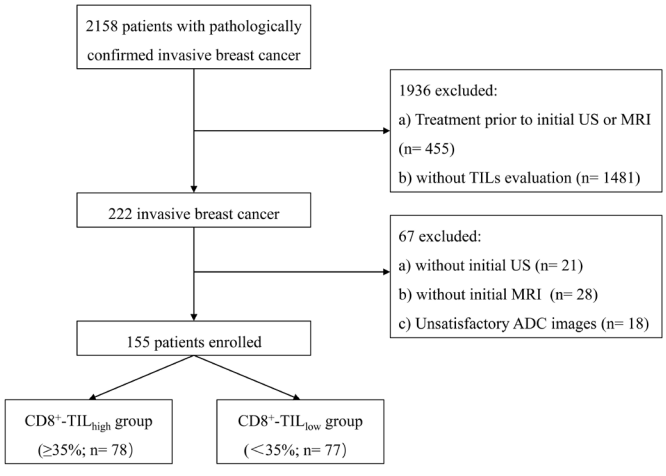

FIG. 1. The flowchart for participant selection.

US, ultrasound; MRI, magnetic resonance imaging; TIL, tumor-infiltrating lymphocytes.

MRI protocol and analysis

Breast MRI was performed using a 1.5-T scanner (Magnetom Aera, Siemens Healthcare, Erlangen, Germany) with an eight-channel breast coil. The MRI scanning protocol was as follows: (a) axial FL3D-T1-weighted imaging (T1WI), repetition time (TR) = 8.6 ms, echo time (TE) = 4.7 ms, the field of view (FOV) = 360 mm x 360 mm, and slice thickness = 4.0 mm; (b) axial turbo inversion recovery magnitude T2WI with fat saturation ($T2WI_{FS}$), TR = 5,600 ms, TE = 57 ms, FOV = 340 mm x 340 mm, and slice thickness = 4.0 mm; (c) axial diffusion-weighted imaging (DWI) using spin echo-echo planar imaging sequence, TR = 6,300 ms, TE = 68 ms, FOV = 340 mm x 159 mm, and b = 0, 50, and 1,000 s/mm^2; and (d) dynamic contrast-enhanced (DCE)-MRI was performed with a 3D fat-suppressed T1 fast-field echo sequence before and five times after intravenous administration of contrast agent (Magnevist, Bayer Healthcare, Berlin, Germany). The total acquisition time for DCE-MRI is 369 s, with each phase lasting 49 s. (e) A single-voxel ^{1}H-MRS was performed using a spin echo sequence (TR = 1,500 ms, TE = 100 ms, flip angle = 90°, voxel size = 15 x 15 x 15 mm^3). The raw MRI images were imported into the post-processing workstation, where the choline peak was determined. Conventional MRI features, such as shape (regular or irregular), tumor size (longest diameter), margin (defined or ill-defined), enhancement pattern (homogeneous or heterogeneous), skin and nipple involvement (absent or present), type of time-intensity curve [(TIC); type I (persistent enhancement), type II (plateau pattern), and type III (washout pattern)], and choline were assessed and recorded. All T2WI, DWI, ADC, and DCE-MRI images were exported to DICOM format and imported into RadiAnt software (https://www.radiantviewer.com/). Three non-overlapping regions of interest (ROIs) of identical size (8-10 mm^2) were placed on the image containing the largest diameter of the breast tumor, avoiding the necrotic, cystic region, and hemorrhagic area; the mean ADC value of these ROIs was final ADC of the tumor. Two experienced radiologists evaluated ADC and conventional MRI features while remaining blind to pathology and US findings. The ADC values measured by the two radiologists were used to calculate the interobserver correlation coefficient (ICC). Finally, the ADC values determined by the first radiologist were used in data analysis. When other MRI features differed between the two radiologists, they negotiated to resolve the differences.

Pathological evaluation of CD8$^+$-TILs

All pathology specimens were obtained using crude needle biopsies. Immunohistochemical markers, including estrogen receptor (ER), HER2, progesterone receptor (PR), Ki-67, and hormone receptor (HR) status, were obtained from the electronic pathology system of our hospital. HER2-positive is defined as HER2 immunohistochemistry (IHC) 3$^+$ or HER2 IHC 2$^+$, with additional confirmation of *HER2* gene amplification by fluorescence in situ hybridization. Because CD8-positive lymphocytes are the effector cells capable of eliminating tumor cells and thus the most relevant subtypes of TILs for the immune response to the tumor,[12] we used the percentage of CD8-positive lymphocytes to represent TIL levels. The International TILs Working Group in BC recommended assessing CD8$^+$-TIL levels in the stromal compartment.[25] Paraffin-embedded tumor sections were processed and immunohistochemically stained for CD8 using the anti-CD8 antibody (cat. no. ZA-0508; ZSGB-BIO, Beijing, China). CD8$^+$-TILs were identified by scanning an entire section of each tumor slide at low magnification (50 g) and defined as those showing faint yellow or brown cell membranes. The ratio of CD8-positive cells to total stromal area within the tumor was calculated as a percentage. The CD8$^+$-TILs status of the tumor was determined by calculating the mean percentage of CD8$^+$-TILs from five randomly selected high magnification (200 g) tumor sections (Figure 2). CD8 staining and interpretation were performed independently by two pathologists with 8 and 10 yr of experience in BC pathology. To determine a clinically relevant TIL threshold, in this study, we used the median CD8$^+$-TIL level (35%) as the cut-off point. Patients were divided into two groups: low (< 35%, CD8$^+$-TIL$_{low}$) and high (≥ 35%, CD8$^+$-TIL$_{high}$).

Statistical analysis

Statistical tests were performed using IBM SPSS statistical software version 24 (IBM Corp., Armonk, New York, USA), R language version 4.0.2 (R Core Team, 2020), or Medcalc Statistical Software Version 22 (Medcalc Software Ltd., Ostend, Belgium). Continuous variables were compared using the independent samples two-sided t-test or the Mann-Whitney U test, depending on the data distribution. Categorical variables were expressed as numbers (%) and compared using the chi-squared test or Fisher's exact test. The *p*-values for multiple comparisons were adjusted using Bonferroni's correction. Univariate and multivariate logistic regression analyses were used to identify the optimal features for predicting CD8$^+$-TIL levels. The predictive models were constructed using stepwise multivariate logistic regression analysis. The predictive performance of CD8$^+$-TIL levels based on US and MRI features was determined using receiver operating characteristic (ROC) analysis, respectively. The area under the ROC curve (AUC) was compared using the DeLong test. All comparisons were considered statistically significant at a *p*-value of < 0.05.

RESULTS

Clinical characteristics of patients

The study included 155 patients with HER2-positive BC who underwent US and MRI, with a mean age of 51.68 ± 10.4 (range, 21-77 yr). According to the percentage of CD8$^+$-TILs, 77 of the 155 patients were assigned to the CD8$^+$-TIL$_{low}$ group, and 78 patients were assigned to the CD8$^+$-TIL$_{high}$ group. The CD8$^+$-TIL$_{low}$ and CD8$^+$-TIL$_{high}$ groups did not differ significantly in age (51.57 ± 9.35 vs. 51.79 ± 11.41, $p = 0.894$), location (left/right: 45/32 vs. 38/40, $p = 0.225$), ER ($p = 0.923$), PR ($p = 0.953$), Ki-67 ($p = 0.467$), and HR ($p = 0.569$). The clinical T stage of tumors differed significantly between the CD8$^+$-TIL groups ($p < 0.033$). Demographic and clinical data are shown in Table 1.

Relationship between US and MRI features and CD8$^+$-TIL levels

There was a statistically significant difference in shape (regular vs. irregular, $p < 0.01$), orientation (parallel vs. non-parallel, $p = 0.01$), and posterior echo (attenuated vs. accentuated, $p < 0.01$; attenuated vs. unaltered, $p < 0.01$) between CD8$^+$-TIL$_{low}$ and CD8$^+$-TIL$_{high}$. Margin, internal echo, and microcalcification did not differ significantly between the two groups (Tables 2, 3). Furthermore, multivariate analysis and logistic regression were performed based on the significant variables derived from univariate analysis, which revealed that shape [irregular vs. regular; odds ratio (OR) = 11.63; 95% confidence interval (CI): 3.18-42.73; $p < 0.001$], orientation (non-parallel vs. parallel; OR = 2.72; 95% CI: 1.13-6.48; $p = 0.026$), and posterior echo (accentuated vs. attenuated; OR = 6.334; 95% CI: 2.513-15.963; $p < 0.001$; unaltered vs. attenuated; OR = 5.820; 95% CI: 2.121-15.971; $p = 0.001$) were the independent US predictors (Table 3). Representative US images of BC from either the CD8$^+$-TIL$_{high}$ group or the CD8$^+$-TIL$_{low}$ group were shown in Figure 3.

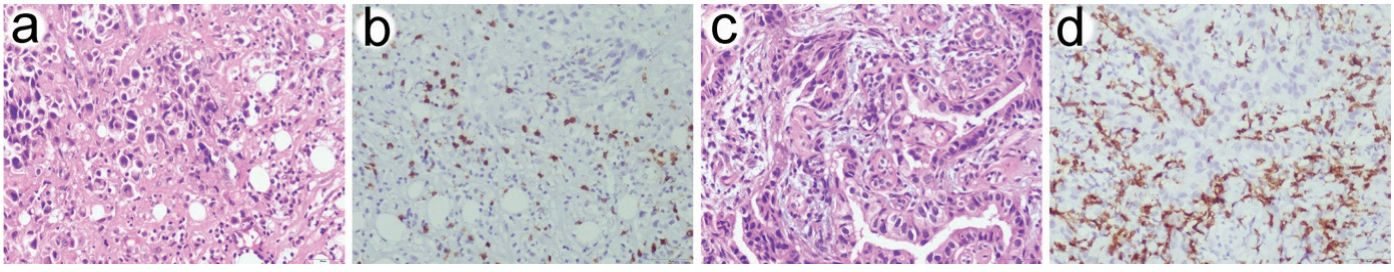

FIG. 2. Histological analysis of HER2-positive BC. (a, b) Breast cancer (BC) with 20% CD8$^+$-TILs (CD8$^+$-TIL$_{low}$). (b-d) BC with 70% CD8$^+$-TILs (CD8$^+$-TIL$_{high}$). (a, c) Hematoxylin-eosin staining (original magnification, × 200 (b, d) CD8-positive lymphocytes-stained images (original magnification, × 200 CD8$^+$-TILs, CD8-positive tumor-infiltrating lymphocytes.

HER2, human epidermal growth factor receptor type 2; TIL, tumor-infiltrating lymphocytes.

TABLE 1. Comparisons of Demographic and Clinical Data in Various $CD8^+$-TIL Groups.

Parameter	$CD8^+$-TIL_{low} (n = 77, 49.7%)	$CD8^+$-TIL_{high} (n = 78, 50.3%)	*z/t*	*p*-value
Age (yr)	51.57 ± 9.35	51.79 ± 11.41	-0.133	0.894
Location (left/right)	45/32	38/40	1.473	0.225
Clinical T stage			6.559	0.033
T1	18 (23.4%)	10 (12.8%)		
T2	52 (67.5%)	66 (84.6%)		
T3	7 (9.1%)	2 (2.6%)		
ER			0.009	0.923
Positive	31 (40.3%)	32 (41.0%)		
Negative	46 (59.7%)	46 (59.0%)		
PR			0.003	0.953
Positive	50 (64.9%)	51 (65.4%)		
Negative	27 (35.1%)	27 (34.6%)		
Ki-67			1.524	0.467
< 14%	11 (14.3%)	7 (9.0%)		
14%-20%	17 (22.1%)	22 (28.2%)		
> 20%	49 (63.6%)	49 (62.8%)		
HR			0.324	0.569
Positive	34 (44.2%)	38 (48.7%)		
Negative	43 (55.8%)	40 (51.3%)		

ER, estrogen receptor; HR, hormone receptor (HR status was defined in terms of ER-positivity and/or PR-positivity as scored by the Allred system, whereby a total score of greater than 2 implies positivity); Ki-67, Ki-67 proliferation index; PR, progesterone receptor; TIL, tumor-infiltrating lymphocytes, T1, tumor ≤ 2 cm; T2, 2 cm < tumor ≤ 5 cm; T3, tumor > 5 cm.

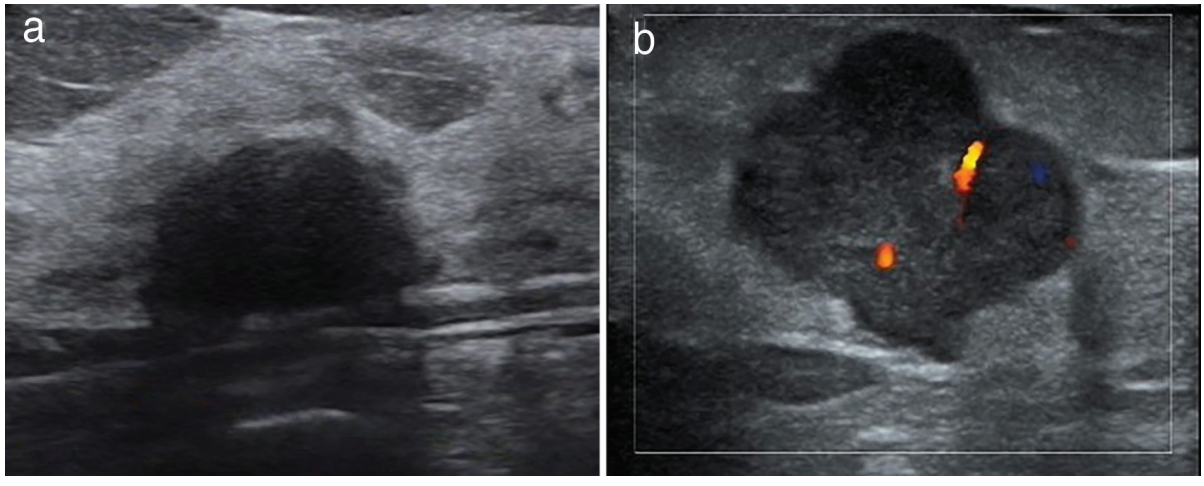

FIG. 3. Representative US images of HER2-positive breast cancer (BC). (a) BC lesion with regular shape, parallel orientation, and attenuated posterior echo. Puncture pathology confirmed a $CD8^+$-TIL level of 21% ($CD8^+$-TIL_{low}). (b) BC lesion with irregular shape, non-parallel orientation, and accentuated posterior echo on ultrasound. Biopsy results confirmed a $CD8^+$-TIL level of 65% ($CD8^+$-TIL_{high}).

US, ultrasound; HER2, human epidermal growth factor receptor type 2; TIL, tumor-infiltrating lymphocytes.

TABLE 2. Comparisons of US and MRI Features in Different $CD8^+$-TIL Groups.

Variables	$CD8^+$-TIL_{low}	$CD8^+$-TIL_{high}	χ^2/z	*p*-value
US features				
Tumor size, M (Q1, Q3), cm	2.61 (2.05, 3.53)	2.80 (2.24, 3.56)	2737.000	0.490
Shape, n (%)			22.807	> 0.001
Regular	26 (33.8%)	3 (3.8%)		
Irregular	51 (66.2%)	75 (96.2%)		
Orientation, n (%)			10.266	0.001
Parallel	65 (84.4%)	48 (61.5%)		
Non-parallel	12 (15.6%)	30 (38.5%)		
Margin, n (%)			2.908	0.088
Defined	36 (46.8%)	26 (33.3%)		
Ill-defined	41 (53.2%)	52 (66.7%)		
Microcalcification, n (%)			0.23	0.632
Present	36 (46.8%)	26 (33.3%)		
Absent	41 (53.2%)	52 (66.7%)		
Internal echoes, n (%)			3.518	0.172
Equal	11 (14.3%)	10 (12.8%)		
Low	62 (80.5%)	57 (73.1%)		
Extremely low	4 (5.2%)	11 (14.1%)		
Posterior echo, n (%)			19.552	< 0.001
Attenuated	36 (46.8%)	11 (14.1%)		
Unaltered	16 (20.8%)	26 (33.3%)		
Accentuated	25 (32.5%)	41 (52.6%)		
MRI features				
Shape, n (%)			0.183	0.669
Regular	10 (13.0%)	12 (15.4%)		
Irregular	67 (87.0%)	66 (84.6%)		
Tumor size, M (Q1, Q3), cm	2.7 (2.15, 4.30)	2.8 (2.20, 4.05)	0.084	0.933
Margin, n (%)			0.031	0.861
Defined	13 (16.9%)	14 (17.9%)		
Ill-defined	64 (83.1%)	64 (82.1%)		
Enhancement pattern			0.776	0.378
Homogenous	41 (53.2%)	46 (60.3%)		
Heterogenous	36 (46.8%)	31 (39.7%)		
Skin involvement			1.090	0.296
Absent	59 (76.6%)	65 (83.3%)		
Present	18 (23.4%)	13 (16.7%)		
Nipple involvement			0.336	0.562
Absent	64 (83.1%)	62 (79.5%)		
Present	13 (16.9%)	16 (20.5%)		
TIC type			2.934	0.231
Type I (persistent enhancement)	8 (10.4%)	3 (3.8%)		
Type II (plateau pattern)	34 (44.2%)	41 (52.6%)		
Type III (washout pattern)	35 (45.5%)	34 (43.6%)		
Cho	38.666 ± 3.399	31.5 (15.2, 50.9)	0.831	0.406
ADC, M (Q1, Q3), mm^2/s	759.650 (693.300, 801.000) x 10^{-6}	816.500 (749.828, 989.250) x 10^{-6}	1551.000	< 0.001

US, ultrasound; MRI, magnetic resonance imaging; TIL, tumor-infiltrating lymphocytes; TIC, time-intensity curve; ADC, apparent diffusion coefficient.

The ICC for ADC values was 0.923 (95% CI: 0.898-0.942), indicating good agreement.

There was a statistically significant positive relationship between ADC and $CD8^+$-TILs (759.650 x 10^{-6} vs. 816.500 x 10^{-6} mm^2/s; $p < 0.001$; Table 2). Tumors in the $CD8^+$-TIL_{high} group were slightly larger on MRI than those in the $CD8^+$-TIL_{low} group, which was consistent with US findings, but the difference was not statistically significant ($p = 0.933$). The choline peak on the ^{1}H-MRS indicates cell proliferation status and is always associated with a higher grade and poor prognosis of the tumor. The $CD8^+$-TIL_{low} group had a higher choline peak than the $CD8^+$-TIL_{high} group; however, there was no statistically significant difference ($p = 0.406$). The enhancement pattern, TIC type, and skin and nipple involvement did not differ significantly between the two groups (Table 2). Representative MR images of BC from either the $CD8^+$-TIL_{high} group or the $CD8^+$-TIL_{low} group were shown in Figure 4.

TABLE 3. Relationship between $CD8^+$-TIL Levels and US Features.

	Univariable analysis			Multivariate analysis		
Variables	**OR**	**95% CI**	**p-value**	**OR**	**95% CI**	**p-value**
Shape						
Regular	1.00			1.00		
Irregular	12.745	3.663-44.347	< 0.001	11.634	3.176-42.618	< 0.001
Orientation						
Parallel	1.00			1.00		
Non-parallel	3.385	1.573-7.285	0.002	2.716	1.129-6.532	0.026
Margin						
Defined	1.00					
Ill-defined	1.756	0.917-3.363	0.089			
Microcalcification						
Present	1.00					
Absent	1.185	0.592-2.374	0.632			
Internal echoes						
Equal	1.00					
Low	1.011	0.399-2.560	0.981			
Extremely low	3.025	0.724-12.632	0.129			
Posterior echogenic						
Attenuated	1.00			1.00		
Unaltered	5.318	2.122-13.326	< 0.001	5.820	2.121-15.971	0.001
Accentuated	5.367	2.320-12.415	< 0.001	6.334	2.513-15.963	< 0.001

TIL, tumor-infiltrating lymphocytes; US, ultrasound; OR, odds ratio; CI, confidence interval.

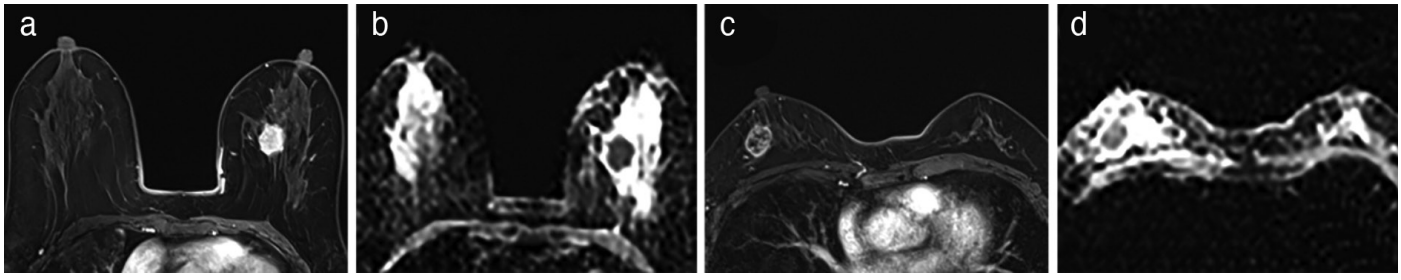

FIG. 4. Representative MRI images of HER2-positive breast cancer (BC). (a, b) BC lesion with an ADC of 694.0 x 10^{-6} mm^2/s in the $CD8^+$-TIL_{low} group. (c, d) BC lesion with an ADC of 1020.2 x 10^{-6} mm^2/s in $CD8^+$-TIL_{high} group. (a, c) Contrast-enhanced images of BC lesions. (b, d) Maps of ADC values. $CD8^+$-TIL_{high}, high $CD8^+$-TILs group; $CD8^+$-TIL_{low}, low $CD8^+$-TIL group.

MRI, magnetic resonance imaging; HER2, human epidermal growth factor receptor type 2; ADC, apparent diffusion coefficient; TIL, tumor-infiltrating lymphocytes.

Predictive performance of US and MRI features

The logistic regression analysis revealed that the ADC was a statistically significant predictor of BC with low or high $CD8^+$-TIL levels (OR = 1.008; 95% CI: 1.005-1.012; $p < 0.001$). ROC analysis revealed that the optimal cutoff value for predicting high $CD8^+$-TIL levels was 849.700 x 10^{-6} mm^2/s, with an AUC of 0.705 (95% CI: 0.624-0.778), sensitivity of 42.47%, and specificity of 94.44% ($z = 4.782$, $p < 0.001$; Figure 5).

ROC analysis was used to evaluate the performance of US features, such as shape, orientation, and posterior echo. Results showed an AUC of 0.802 (95% CI: 0.730-0.861), sensitivity of 91.03%, and specificity of 62.34% ($z = 8.251$, $p < 0.001$). The DeLong test found no significant difference in the AUC of ADC and US features ($z = 1.787$, $p = 0.074$). These findings indicate that US features have comparable performance to ADC value in predicting the $CD8^+$-TIL levels in HER2-positive BC. Because most patients with suspected BC undergo US and MRI examinations before treatment planning in our hospital, we combined ADC value with US features to determine whether the ADC value could provide additional predictive value. The combination of ADC and US features significantly improved predictive performance (AUC = 0.888; 95% CI: 0.825-0.934), outperforming either the US features ($z = 2.618$, $p = 0.009$) or the ADC value alone ($z = 5.041$, $p < 0.001$; Figure 5). The nomogram model that incorporates US features and ADC is shown in Figure 6.

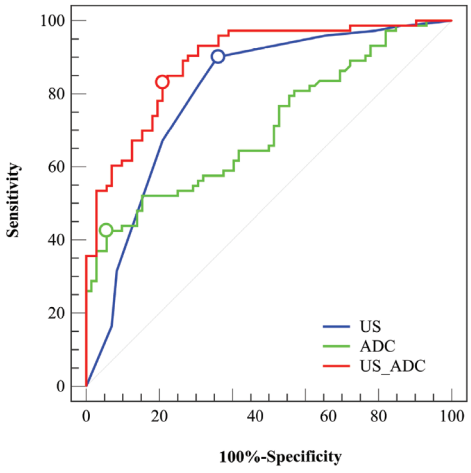

FIG. 5. Receiver operating characteristic curves of models constructed from ADC, US features, and US_ADC, respectively. ADC, apparent diffusion coefficient; US_ADC, combination of US and ADC.

ADC, apparent diffusion coefficient; US, ultrasound.

DISCUSSION

Several studies have demonstrated the effectiveness of US[13-16] and MRI[1-5,10,11,14,17-24] in predicting TILs in BC. However, only one study has evaluated TILs in BC in multimodality (US and MRI).[14] To the best of our knowledge, this paper is the first to analyze US and MRI in the evaluation of $CD8^+$-TILs in HER2-positive BC. In this study, we found that US features (including shape, orientation, and posterior echo) and ADC values have good performance in predicting $CD8^+$-TIL levels in HER2-positive BC, and the predictive ability of US features and ADC values were comparable. Furthermore, when predicting $CD8^+$-TIL levels in HER2-positive BC, the combination of US features and ADC values outperforms either US features or ADC values alone.

Previous studies indicate that the group with high TILs in BC is more likely to exhibit traditional US features, such as round and oval shape (as opposed to irregular shape),[13-15] well-defined margin (as opposed to burr-like margin, microlobular morphology, and blurred margin),[13-15] accentuated posterior echo (as opposed to attenuated posterior echo),[15,16] maximum diameter of ≥ 2 cm,[14] lobulated (as opposed to round and oval),[16] hypoechoic nodules (as opposed to isoechoic and hyperechoic nodules),[16] and complex cystic echogenic nodules and homogeneous hypoechoic nodules (as opposed to inhomogeneous echogenic nodules).[15] There are

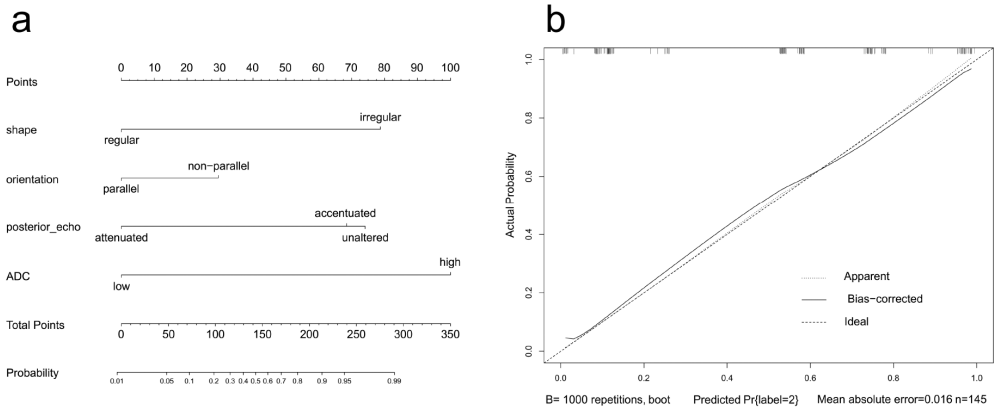

FIG. 6. (a) Nomogram shows the logistic model of US_ADC for prediction of $CD8^+$-TILs in HER2-positive breast cancer. Predictive nomogram for $CD8^+$-TILs incorporating shape, orientation, posterior echo, and ADC. (b) Calibration curves of the logistic model of US_ADC for predicting $CD8^+$-TIL levels in HER2-positive breast cancer.

ADC, apparent diffusion coefficient; US, ultrasound; HER2, human epidermal growth factor receptor type 2; TIL, tumor-infiltrating lymphocytes.

also differing views on some of the US features mentioned above. Jia et al.[13] found that neither internal echogenic characteristics nor maximum nodule diameter were statistically significant predictors of TIL levels in BC. Our study found that BC in $CD8^+$-TIL_{high} were more likely to have an irregular shape. This is consistent with the findings of Fukui et al.[16] but differs from three other studies.[13-15] Although orientation was not statistically significant in predicting TIL levels in the previous two studies,[13,16] it was still a valid predictor of $CD8^+$-TIL levels in our study. This could be explained by the fact that the percentage of CD8-positive lymphocytes in our study served as the predictive population. In our study, HER2-positive BC with higher levels of $CD8^+$-TILs had an irregular shape and non-parallel orientation, which could be attributed to the fact that high TIL cells inflate and expand the angular margins of BC nodules, exhibiting a lobulated morphology.[16] Previous studies indicate that BC in the high TIL group are hypoechoic[16] with a maximum diameter of ≥ 2 cm.[14] However, in the present study, there was no significant difference in internal echogenicity or tumor maximum diameter between the $CD8^+$-TIL_{low} and $CD8^+$-TIL_{high} groups, which is consistent with the findings of Jia et al.[13]

Based on the univariate analysis, the variables of shape, orientation, and posterior echo were examined using multivariate logistic regression. The results show that the shape, orientation, and posterior echo are independent predictors of TIL levels. ROC analysis revealed that these US features were highly predictive, with an AUC of 0.802 and sensitivity and specificity of 91.03% and 62.34%, respectively. This diagnostic efficacy was comparable with that of the prediction model developed by Jia et al.[13] (AUC = 0.79) and Su et al.[26] (AUC = 0.79) but slightly lower than that of the model developed by Fukui et al.[16] (AUC = 0.88). The above results indicate that a predictive model based on US features is highly valuable for determining the level of $CD8^+$-TILs in HER2-positive BC.

Several studies have investigated the relationship between MRI features and TILs in BC,[1-4,10,14,17-20,22-24] but the results have been insufficient. Different cellular and stromal components within the tumor may affect the average ADC of the neoplastic lesion.[20,27] Our results found a significant positive relationship between ADC value and $CD8^+$-TILs in HER2-positive BC (cut-off: 849.700 x 10^{-6} mm^2/s; AUC = 0.705). This is consistent with the results of previous studies.[3,14,20] However, there have been conflicting results. Bian et al.[18] concluded that the relationship between ADC and TILs in BC was not significant, whereas Lee et al.[1] found that ADC was significantly negatively correlated with TILs in BC. Except for ADC values, no other MRI features (such as shape, tumor size, margin, enhancement pattern, skin involvement, nipple involvement, TIC type, and choline) were found to be associated with $CD8^+$-TIL levels. However, these characteristics may differ significantly from previous literature in terms of TIL levels. Previous findings have found that BC lesions with high TIL levels appear on MRI images as round,[14,24] large size,[3] well-defined margins,[14,24] and homogeneous enhancement patterns.[3,14,24] There are several possible reasons for the difference between studies. First, consider various cutoff values used to group TILs. Second, TIL levels are affected by various pathologies of BC.[14] Third, unlike previous studies, this study focused on the relationship between MRI features and $CD8^+$-TIL levels in HER2-positive BC. Finally, the ROI for measuring ADC values was manually delineated and artificially located, which may result in differences.

Our study found that the US features and ADC values performed similarly in predicting $CD8^+$-TIL levels (0.802 vs. 0.705, $p = 0.104$). To determine whether ADC values could improve diagnostic performance, we developed a combined model using US features and ADC values. Indeed, the combined model showed better diagnostic performance than US and ADC values alone, with an AUC of 0.890. This result indicates that the combination of US features and ADC values can accurately predict $CD8^+$-TIL levels in HER2-positive BC.

This study has several limitations. First, this study did not investigate the relationship between $CD8^+$-TILs and pathological complete response and disease-free survival. Second, $CD8^+$-TIL levels were determined using biopsy samples, which could introduce sample bias due to intratumoral heterogeneity. Finally, this study was retrospective and included patients from a single research group, resulting in a small sample size. More research with a large sample size is needed to validate the efficacy of the model in distinguishing the levels of CD8-positive lymphocytes in HER2-positive BC.

The level of TILs is a reliable surrogate for evaluating the prognosis of BC. However, it remains challenging to assess TILs non-invasively before surgery. HER2-positive BC patients with US features (irregular shape, non-parallel orientation, and accentuated or unaltered posterior echo) and higher ADC values may have higher $CD8^+$-TIL levels. The multimodal-based nomogram could help clinicians make decisions.

Acknowledgements: We would like to express our sincere gratitude to all the medical staff of the Department of Ultrasound Diagnosis for their dedication and professionalism in performing the ultrasound examinations. We also thank all the people who have supported and helped us in this research, including the doctors from departments of Breast and Thyroid Surgery, Radiology, and Pathology, who provided us with the clinical data and specimens. Their valuable comments and suggestions have greatly improved the quality of our work.

Ethics Committee Approval: This study was approved by the Ethics Committee of Army Medical Hospital [approval number: 2023 (202)].

Data Sharing Statement: The data that support the findings of this study are available from the corresponding author upon reasonable request.

Authorship Contributions: Concept- Y.F., J.F.; Design- Y.F., J.F.; Supervision- J.F.; Fundings- J.F.; Materials- Y.F., X.L., P.Z., H.G., D.H., W.T., J.F.; Data Collection or Processing- Y.F., X.L., J.F.; Analysis or Interpretation- Y.F., J.F.; Literature Search- J.F.; Writing- Y.F.; Critical Review- Y.F., X.L., P.Z., H.G., D.H., W.T., J.F.

Conflict of Interest: The authors declare that they have no conflict of interest.

Funding: This work was supported by the Innovation Ability Enhancement Project of Daping Hospital - Multimodal ultrasound in BI-RADS category 4 breast mass grading diagnosis and prognostic assessment of breast cancer (Grant Number: ZXZYTSLC07), and Natural Science Foundation of Chongqing, China (Grant Number: cstc2021jcyj-msxmX0230).

REFERENCES

1. Lee HJ, Lee JE, Jeong WG, et al. HER2-Positive Breast Cancer: Association of MRI and Clinicopathologic Features with Tumor-Infiltrating Lymphocytes. *AJR Am J Roentgenol.* 2022;218:258-269. [CrossRef]
2. Choi WJ, Kim Y, Cha JH, et al. Correlation between magnetic resonance imaging and the level of tumor-infiltrating lymphocytes in patients with estrogen receptor-negative HER2-positive breast cancer. *Acta Radiol.* 2020;61:3-10. [CrossRef]
3. Chen S, Sui Y, Ding S, et al. A simple and convenient model combining multiparametric MRI and clinical features to predict tumour-infiltrating lymphocytes in breast cancer. *Clin Radiol.* 2023;78:1065-1074. [CrossRef]
4. Xu N, Zhou J, He X, et al. Radiomics Model for Evaluating the Level of Tumor-Infiltrating Lymphocytes in Breast Cancer Based on Dynamic Contrast-Enhanced MRI. *Clin Breast Cancer.* 2021;21:440-449. [CrossRef]
5. Yoon GY, Chae EY, Cha JH, et al. Imaging and Clinicopathologic Features Associated with Pathologic Complete Response in HER2-positive Breast Cancer Receiving Neoadjuvant Chemotherapy With Dual HER2 Blockade. *Clin Breast Cancer.* 2020;20: 25-32. [CrossRef]
6. Hamy AS, Bonsang-Kitzis H, De Croze D, et al. Interaction between Molecular Subtypes and Stromal Immune Infiltration before and after Treatment in Breast Cancer Patients Treated with Neoadjuvant Chemotherapy. *Clin Cancer Res.* 2019;25:6731-6741. [CrossRef]
7. Stanton SE, Adams S, Disis ML. Variation in the Incidence and Magnitude of Tumor-Infiltrating Lymphocytes in Breast Cancer Subtypes: A Systematic Review. *JAMA Oncol.* 2016;2:1354-1360. [CrossRef]
8. Valenza C, Taurelli Salimbeni B, Santoro C, Trapani D, Antonarelli G, Curigliano G. Tumor Infiltrating Lymphocytes across Breast Cancer Subtypes: Current Issues for Biomarker Assessment. *Cancers (Basel).* 2023;15:767. [CrossRef]
9. Savas P, Salgado R, Denkert C, et al. Clinical relevance of host immunity in breast cancer: from TILs to the clinic. *Nat Rev Clin Oncol.* 2016;13:228-241. [CrossRef]
10. Murakami W, Tozaki M, Sasaki M, et al. Correlation between (18)F-FDG uptake on PET/MRI and the level of tumor-infiltrating lymphocytes (TILs) in triple-negative and HER2-positive breast cancer. *Eur J Radiol.* 2020;123:108773. [CrossRef]
11. Jeon SH, Kim SW, Na K, Seo M, Sohn YM, Lim YJ. Radiomic models based on magnetic resonance imaging predict the spatial distribution of CD8+ tumor-infiltrating lymphocytes in breast cancer. *Front Immunol.* 2022;13:1080048. [CrossRef]
12. Krijgsman D, van Leeuwen MB, van der Ven J, et al. Quantitative Whole Slide Assessment of Tumor-Infiltrating CD8-Positive Lymphocytes in ER-Positive Breast Cancer in Relation to Clinical Outcome. *IEEE J Biomed Health Inform.* 2021;25:381-392. [CrossRef]
13. Jia Y, Zhu Y, Li T, et al. Evaluating Tumor-Infiltrating Lymphocytes in Breast Cancer The Role of Conventional Ultrasound and Contrast-Enhanced Ultrasound. *J Ultrasound Med.* 2023;42:623-634. [CrossRef]
14. Çelebi F, Agacayak F, Ozturk A, et al. Usefulness of imaging findings in predicting tumor-infiltrating lymphocytes in patients with breast cancer. *Eur Radiol.* 2020;30:2049-2057. [CrossRef]
15. Candelaria RP, Spak DA, Rauch GM, et al. BI-RADS Ultrasound Lexicon Descriptors and Stromal Tumor-Infiltrating Lymphocytes in Triple-Negative Breast Cancer. *Acad Radiol.* 2022;29(Suppl 1):35-41. [CrossRef]
16. Fukui K, Masumoto N, Shiroma N, et al. Novel tumor-infiltrating lymphocytes ultrasonography score based on ultrasonic tissue findings predicts tumor-infiltrating lymphocytes in breast cancer. *Breast Cancer.* 2019;26:573-580. [CrossRef]
17. Tang WJ, Kong QC, Cheng ZX, et al. Performance of radiomics models for tumour-infiltrating lymphocyte (TIL) prediction in breast cancer: the role of the dynamic contrast-enhanced (DCE) MRI phase. *Eur Radiol.* 2022;32:864-875. [CrossRef]
18. Bian T, Wu Z, Lin Q, et al. Evaluating Tumor-Infiltrating Lymphocytes in Breast Cancer Using Preoperative MRI-Based Radiomics. *J Magn Reson Imaging.* 2022;55:772-784. [CrossRef]
19. Jimenez JE, Abdelhafez A, Mittendorf EA, et al. A model combining pretreatment MRI radiomic features and tumor-infiltrating lymphocytes to predict response to neoadjuvant systemic therapy in triple-negative breast cancer. *Eur J Radiol.* 2022;149:110220. [CrossRef]
20. Fogante M, Tagliati C, De Lisa M, Berardi R, Giuseppetti GM, Giovagnoni A. Correlation between apparent diffusion coefficient of magnetic resonance imaging and tumor-infiltrating lymphocytes in breast cancer. *Radiol Med.* 2019;124:581-587. [CrossRef]
21. Braman N, Prasanna P, Whitney J, et al. Association of Peritumoral Radiomics With Tumor Biology and Pathologic Response to Preoperative Targeted Therapy for HER2 (ERBB2)-Positive Breast Cancer. *JAMA Netw Open.* 2019;2:e192561. [CrossRef]
22. Wu J, Li X, Teng X, et al. Magnetic resonance imaging and molecular features associated with tumor-infiltrating lymphocytes in breast cancer. *Breast Cancer Res.* 2018;20:101. [CrossRef]
23. Ku YJ, Kim HH, Cha JH, et al. Predicting the level of tumor-infiltrating lymphocytes in patients with triple-negative breast cancer: Usefulness of breast MRI computer-aided detection and diagnosis. *J Magn Reson Imaging.* 2018;47:760-766. [CrossRef]
24. Ku YJ, Kim HH, Cha JH, et al. Correlation Between MRI and the Level of Tumor-Infiltrating Lymphocytes in Patients With Triple-Negative Breast Cancer. *AJR Am J Roentgenol.* 2016;207:1146-1151. [CrossRef]
25. Salgado R, Denkert C, Demaria S, et al. The evaluation of tumor-infiltrating lymphocytes (TILs) in breast cancer: recommendations by an International TILs Working Group 2014. *Ann Oncol.* 2015;26:259-271. [CrossRef]
26. Su GH, Xiao Y, Jiang L, et al. Radiomics features for assessing tumor-infiltrating lymphocytes correlate with molecular traits of triple-negative breast cancer. *J Transl Med.* 2022;20:471. [CrossRef]
27. Chen L, Liu M, Bao J, et al. The correlation between apparent diffusion coefficient and tumor cellularity in patients: a meta-analysis. *PLoS One.* 2013;8:e79008. [CrossRef]